Atmos. Chem. Phys., 12, 10107–10123, 2012
www.atmos-chem-phys.net/12/10107/2012/
doi:10.5194/acp-12-10107-2012

Atmospheric Chemistry and Physics

Analysis of exceedances in the daily PM_{10} mass concentration ($50\,\mu g\,m^{-3}$) at a roadside station in Leipzig, Germany

C. Engler, W. Birmili, G. Spindler, and A. Wiedensohler

Leibniz-Institute for Tropospheric Research, Leipzig, Germany

Correspondence to: C. Engler (engler@tropos.de)

Received: 13 May 2011 – Published in Atmos. Chem. Phys. Discuss.: 25 May 2011
Revised: 9 October 2012 – Accepted: 10 October 2012 – Published: 5 November 2012

Abstract. Five years of PM_{10} and $PM_{2.5}$ ambient air measurements at a roadside, an urban, and a regional background site in Leipzig (Germany) were analyzed for violations of the legal PM_{10} limit value (EC, 1999). The annual mean PM_{10} concentrations at the three sites were well below the legal threshold of $40\,\mu g\,m^{-3}$ (32.6, 22.0 and $21.7\,\mu g\,m^{-3}$, respectively). At roadside, the daily maximum value of $50\,\mu g\,m^{-3}$ was exceeded on 232 days (13 % of all days) in 2005–2009, which led to a violation of the EC directive in three out of five years. We analysed the meteorological factors and local source contributions that eventually led to the exceedances of the daily limit value. As noted in other urban environments before, most exceedance days were observed in the cold season. Exceedance days were most probable under synoptic situations characterised by stagnant winds, low temperatures and strong temperature inversions in winter time. However, these extreme situations accounted for only less than half of the exeedance days. We also noticed a significant number of exceedance days that occurred in the cold season under south-westerly winds, and in the warm season in the presence of easterly winds. Our analysis suggests that local as well as regional sources of PM are equally responsible for exceedances days at the roadside site. The conclusion is that a combined effort of local, national and international reduction measures appears most likely to avoid systematic exceedances of the daily limit value in the future.

1 Introduction

Since 2005, legal limit values apply to environmental particulate matter (PM) within the European Community (EC, 1996, 1999). PM_{10} denotes the total mass concentration of suspended particles with aerodynamic diameters smaller than 10 µm. The metrics of PM_{10} and $PM_{2.5}$ are simple in that they can be determined in air quality networks with reasonable costs using on-line instrumentation such as the TEOM (tapered element oscillating microbalance), the beta gauge, the OPC (optical particle counter), or the off-line reference methods based on filter collection and gravimetry.

On the other hand, it is evident that especially PM_{10} encompasses a wide range of particle types regarding size (coarse, fine, ultrafine), chemical composition (dust, combustion particles, marine primary particles, secondary organic aerosol, secondary inorganic aerosol), and sources (natural, traffic, industry, domestic households, secondary processes). This complex composition hampers the understanding of PM_{10} as a function of local sources, long-range transport and meteorology for a given site. In practice, exceedances of the legal limit values, particularly the daily limit value of $50\,\mu g\,m^{-3}$ have frequently occurred at air quality monitoring stations in many EC member states. Due to the scientific evidence of health effects as a result of airborne particulate matter exposure, health effects scientists have called for a more serious consideration of efficient abatement measures (Annesi-Maesano et al., 2007).

The actual reasons for the PM_{10} exceedances are manifold on a European and worldwide level. In the UK, which may be taken as representative for Western Europe, the advection of continental air masses as well as regional secondary aerosol formation seem to be responsible for the majority of exceedances (Charron et al., 2007). In the metropolitan area of Berlin, Germany, 50 % of the PM_{10} mass concentration is estimated to originate from regional and long-range transport rather than local sources (Lenschow et al., 2001). In arid regions like Spain, wind-blown mineral dust – partially

imported from Africa, partially from agricultural soils, may have a major impact (Escudero et al., 2007). Even as far north as Germany, Saharan dust may enhance PM concentrations at ground level several times a year (Bruckmann et al., 2008).

Agricultural dust is sometimes assumed to be responsible for the differences between measured and modelled PM_{10} concentrations in urban areas, and significant amounts thereof can originate from long-range transport (Vautard et al., 2005; Birmili et al., 2008). Putaud et al. (2010) concluded for Europe that mineral aerosol is the main component in the $PM_{[2.5;10]}$ aerosol fraction, but of minor importance in $PM_{2.5}$. Particular sources of PM_{10} in urban environments are traffic, domestic heating and cooking, construction sites, industries, power generation or wind-blown resuspended dust (e.g., Querol et al., 2004). The traffic induced contribution includes abrasion (e.g., brake wear and tyre wear) (Sanders et al., 2003; Weckwerth, 2001), resuspension of road dust (Sternbeck et al., 2002; Amato et al., 2009), diesel soot particles (Kittelson, 1998; Rose et al., 2006) and nucleation mode particles (Kittelson, 1998) from exhaust gas.

According to official inventories, the emissions of primary particles and precursors of secondary particles in Europe have declined significantly over the past 20 yr, particularly in Central and Eastern Europe as a result of political and economic changes since 1990. Until the year 2000, these emission reductions have reflected themselves in clear corresponding trends of PM_{10}, for example in Germany (Spindler et al., 2004; UBA, 2009). Since the year 2000, however, the PM_{10} concentrations in Germany seem to stagnate, and feature some mere inter-annual fluctuations (UBA, 2009). A similar stagnation of PM_{10} since 2000 has also been reported for other areas in Europe, such as the UK (Harrison et al., 2008), Switzerland (Barmpadimos et al., 2011), Belgium, Czech Republic, Italy and Norway. This is in notable contrast to the continued reductions in PM emissions. Germany, for example, reported a 20 % decrease in PM_{10} emissions between 2000 and 2010 (updated information from UBA (2009)). The stagnating ambient levels of PM_{10} are therefore not fully understood and merit detailed examination. A better understanding on the sources and concentrations of PM_{10} is highly relevant, because the problem of exceedances in the daily limit value of PM_{10} seem to continue.

This work is concerned with the analysis of the meteorological situations leading to exceedances of the daily limit value of PM_{10} ($50\,\mu g\,m^{-3}$) in the city of Leipzig, East Germany. The main tool is back trajectory cluster analysis. In order to minimize subjectivity, a *k*-means cluster algorithm was applied in this study. Trajectory coordinates were used as the clustering variables the first time by Moody and Galloway (1988). Also, Kemp (1993) and Mukai and Suzuki (1996) have analysed aerosol data using air mass trajectories. Ozone concentration data have been interpreted by trajectory clustering methods by Brankov et al. (1998) or Cape et al. (2000). The long-range transport of aerosol particle concentrations was estimated by Buchanan et al. (2002), and Dutkiewicz et al. (2004) investigated the long-range transport of sulphate. Similar to the procedure presented here, Abdalmogith and Harrison (2005) clustered back trajectories and then assigned pollutant concentrations like PM_{10} to the defined clusters. They found the highest sulfate, nitrate and PM_{10} mass concentrations and the lowest chloride mass concentrations in continental air masses and reversely the lowest ones in fast moving marine air masses. Higher particle mass concentrations were also observed in winter and spring compared to summer and fall. Beddows et al. (2009) applied a completely mathematical cluster analysis without the use of back trajectories for rural, urban and, kerbside atmospheric particle size data to determine temporal and spatial trends of the particle size distributions. Baker (2010) used a cluster analysis to analyze the long-range air transport and associated particle mass concentrations. The cluster method used here was already successfully applied for the interpretation of transboundary anthropogenic pollution (Engler et al., 2007; Birmili et al., 2010).

2 Experimental

2.1 Observation sites

In this work, PM_{10} mass concentrations and exceedances of the daily limit value of $50\,\mu g\,m^{-3}$ were analyzed for the city of Leipzig, Germany, for the period between January 2005 and December 2009. The observation sites include a roadside site ("Leipzig-Mitte") and an urban background site ("Leipzig-West") operated by the Saxon State Office for Environment, Agriculture and Geology. To assess the regional background of PM we employed data from IfT's research station Melpitz, around 50 km northeast of Leipzig.

Leipzig-Mitte is a roadside site in Leipzig, located near the inner-city ring road and in immediate vicinity to the central train station (Fig. 1). Among the three stations, Leipzig-Mitte exhibits the highest concentrations of particulates and nitrogen oxides. Immediately north of the site, three main roads merge at an intersection with daily average traffic volumes around 44 000 vehicles (48 000 on workdays) in 2008. The measurement container borders at a tributary road connected to the ring road by traffic lights. This sometimes leads to traffic jams at only few meters distance to the aerosol inlets of the measurement site. Construction activities in the vicinity of the site have occasionally disturbed the measurements in 2007 and 2008. The influence of these constructions was estimated to contribute around $10\,\mu g\,m^{-3}$ to the monthly average of PM_{10} for December 2007 and January 2008, respectively (The City of Leipzig, 2009).

Leipzig-West is located in the western suburbans of Leipzig, and is classified as an urban background station. The distance to Leipzig-Mitte is about 7 km. The residential area consists of multi-storey apartment blocks that are heated by

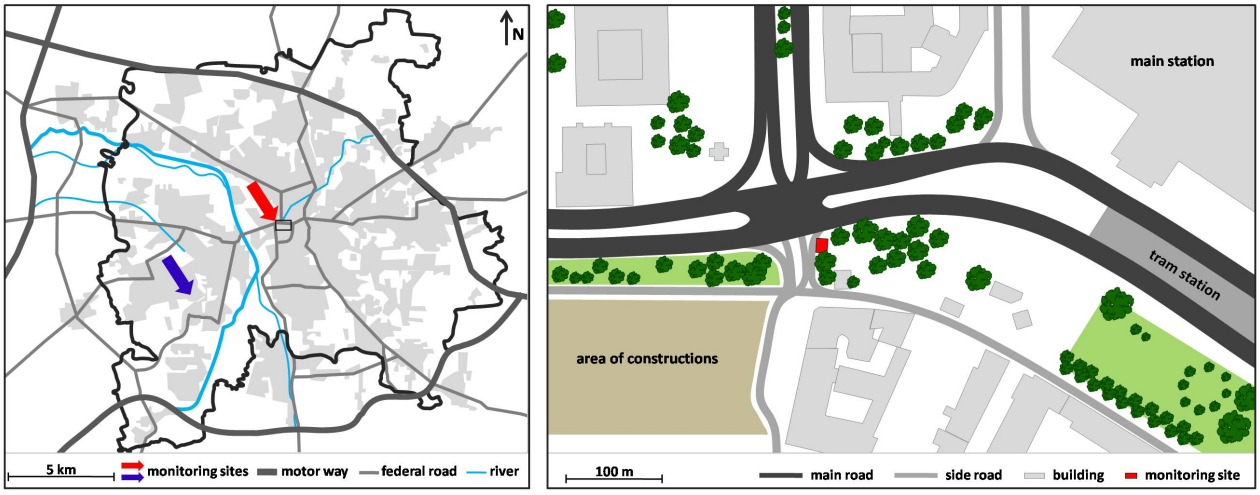

Fig. 1. Regional map of Leipzig, Germany, including the detailed surroundings of the LfULG monitoring site Leipzig-Mitte.

district heating. The station is installed on hospital premises, with the vicinity being dominated by a green park. A minor road passes by the station around 30 m west of the site.

Melpitz is a research station located about 50 km northeast of Leipzig. The site is surrounded by flat grass lands, agricultural pastures and woodlands within several tens kilometres. The measurement site can be considered as representative for the Central European regional aerosol (Engler et al., 2007; Spindler et al., 2010). The overall distance to the North Sea is about 400 km to the northwest and 1000 km to the west. Melpitz is part of the networks ACTRIS (Aerosols, clouds, and trace gases research Infrastructure network), EMEP (European Monitoring and Evaluation Programme) and GUAN (German Ultrafine Aerosol Network; Birmili et al., 2009).

2.2 PM measurements

The 24 h mass concentrations of PM_{10} and $PM_{2.5}$ at Leipzig-Mitte and Melpitz were determined by using Digitel High Volume Samplers (Walter Riemer Messtechnik, Germany) (Gnauk et al., 2005). PM_{10} mass in Leipzig-Mitte and Melpitz as well as $PM_{2.5}$ in Melpitz were available daily, but $PM_{2.5}$ in Leipzig-Mitte only every second day. For Leipzig-Mitte, glass-fibre filters were used. Because the 24 h filter samples of Melpitz were additionally analyzed for daily chemical particle composition considering the main ions (sulfate, nitrate, ammonium, chloride, sodium, calcium, magnesium, potassium) and organic and elemental carbon, the use of quartz-fibre filters was mandatory.

These quartz-fibre filters were preheated for 24 h at 105°C to minimize blank values of OC (Spindler et al., 2010). The conditioning time before weighing was 48 h (relative humidity 50(±2) %, temperature 20(±2) °C). The uncertainty for the gravimetrical mass determination is about 1 to 2 $\mu g\,m^{-3}$ and for the ion analysis less than 10 % (Neusüß et al., 2000; Brüggemann et al., 2005).

In Leipzig-West, PM_{10} mass concentrations were measured with the standard TEOM instrument (Tapered Element Oscillating Microbalance) at a time resolution of 30 min. This method is biased, because the standard operation temperature of 50 °C causes a systematic underestimation of the real PM_{10} values of up to 50 % due to the evaporation of volatile compounds such as ammonium nitrate (Charron et al., 2004; Spindler et al., 2010). As a general correction scheme, the TEOM values at Leipzig-West were adjusted by the network operator by using a limited set of samples determined by the reference method. The correction scheme involved a multiple regression analysis using ambient temperature and relative humidity as control variables. While the mean values obtained by that method for Leipzig-West can be considered reliable, individual daily values may be afflicted with considerable uncertainty.

2.3 Auxiliary data

Local meteorological measurements were conducted at all three observation sites. In addition, 72 h back trajectories were calculated using the NOAA-HYSPLIT4 (HYbrid Single-Particle Lagrangian Integrated Trajectory) model (Draxler and Hess, 2004). Radio soundings from the meteorological observatory Lindenberg, operated by the German Weather Service (DWD), were used in the trajectory cluster analysis. Lindenberg is situated about 150 km northeast of Leipzig and the profiles obtained there are assumed to be representative for Leipzig as well due to the flat terrain in between.

3 Data processing methods

All PM data were processed as daily average values (sampling time 00:00–24:00 CET). Based on the daily PM_{10} mass

concentration, each measurement day was classified into an exceedance or a non-exceedance day according to the EC directive 1999/30/EC.

3.1 Derivation of the roadside increment

Lenschow et al. (2001) showed for the metropolitan region of Berlin that PM_{10} concentration at a roadside (or traffic kerbside) can be described as a superposition of three source type contributions: (a) the regional background, (b) the urban background increment, which originates from sources inside the same city, but not from immediately nearby, and (c) the roadside increment which originates from vehicular traffic on the adjacent road or street. Lenschow et al. (2001) estimated these contributions by subtracting roadside, urban background, and rural background concentrations, respectively. In this paper, we mostly use the roadside increment $\Delta\,PM_{10}$ in the definition of

$$\Delta\,PM_{10} = PM_{10,\mathrm{roadside}} - PM_{10,\mathrm{rural}}. \quad (1)$$

The reason for omitting the urban background concentrations were twofold. First, there is a close agreement between urban and rural background PM_{10} concentrations in Leipzig, as shown in Sect. 4.1. This leads to the urban background being around zero most of the time. Second, we face a reduced measurement accuracy for PM_{10} at the urban backgrund station due to the use of a standard TEOM, as explained in Sect. 2.2. These reasons prohibit a sound interpretation of the urban background increment within the measurement accuracy.

3.2 Back trajectory cluster analysis

Back trajectories have been recognized as a valuable tool to investigate the large-scale origin of air pollutants (Stohl, 1998). Back trajectory cluster analysis combines similar trajectories into distinct groups (clusters). One major advantage of the cluster method is that it can be automated.

We applied a custom-made k-means cluster algorithm (programmed in LabVIEW, National Instruments, Version 6.1), which was developed in analogy to the approach first reported by Dorling et al. (1992). k-means cluster analysis divides the data set into a predetermined number k of trajectory clusters. The groundwork of the cluster analysis were back trajectories calculated using the HYSPLIT4 model. In addition, vertical profiles of pseudo potential temperature Θ_e calculated from 12:00 UTC radiosonde ascents were used. Profiles of pseudo potential temperature were incorporated in the cluster variables because they characterize the degree of vertical atmospheric stratification, which is of vital importance for pollutant dispersal near the ground. We successfully applied this cluster method before (Engler et al., 2007; Birmili et al., 2010), and confirmed that the inclusion of the vertical temperature profile enhanced the meaningfulness of the cluster results, particularly when using multi-annual time series.

The following Euclidian distances were computed to express the spatial separation between two back trajectories i and j:

$$L_{i,j} = \frac{1}{k}\sum_{k}\sqrt{\sum_{l=1}^{4} a_l (x_{li} - x_{lj})^2}. \quad (2)$$

Here, k is the number of trajectory points, which was chosen as $k = 72$ to represent hourly back trajectory positions over 3 days. The choice of back trajectory length of 72 h was supported by the life time of several secondary species (Wojcik and Chang, 1997).

l is the dimension of the vector to be clustered, which includes the four variables of geographical latitude and longitude (x, y; both in Cartesian coordinates), height above ground (z) and pseudo potential temperature (Θ_e). To create four variables of equitable magnitude, the weights a_l are required and were chosen as $a_1 = a_2 = 1\,^{\circ\,-1}$, $a_3 = 10^{-5}\,\mathrm{m}^{-1}$, and $a_4 = 2\,\mathrm{K}^{-1}$.

Notably, the choice of a_3 and a_4 required prior test runs, because temperature is a variable entirely dissimilar from geographical position. In practice, the cluster algorithm was run for a range of cluster numbers between 3 and 14. The deviation of the average PM_{10} concentrations (and the other aerosol and meteorological data) between the clusters was calculated for each test run and used for the choice of the weighing parameters. A higher pre-defined cluster number will split the data set in smaller sub-sets, which correspond more specifically to certain synoptic-scale weather situations. A lower cluster number will, in contrast, produce less but larger sub-sets of data. Those larger sub-sets may be representative for larger parts of the entire observation period, but are less specific to individual synoptic-scale weather situations. The decision, how many clusters to use for the final discussion of the PM_{10} data reflected a compromise between simplicity of display (low n) and a more visible separation of the data clusters (high n), and yielded in 9 clusters.

4 Results

4.1 Basic characteristics of PM_{10} in Leipzig

Figure 2 presents the time series of PM_{10} concentration at the three observation sites (roadside, urban background, rural) throughout the entire observation period 2005–2009. The sites were characterised by long-term averages between 21 and 33 $\mu\mathrm{g\,m}^{-3}$. See Table 1 for a brief overview of the PM_{10} and $PM_{2.5}$ mean values. These PM_{10} concentrations are consistent with other Central European lowland observation sites whose annual average values range between 20 and 30 $\mu\mathrm{g\,m}^{-3}$ (Putaud et al., 2010). It is worth to note that in every year, there is at least one longer episode with

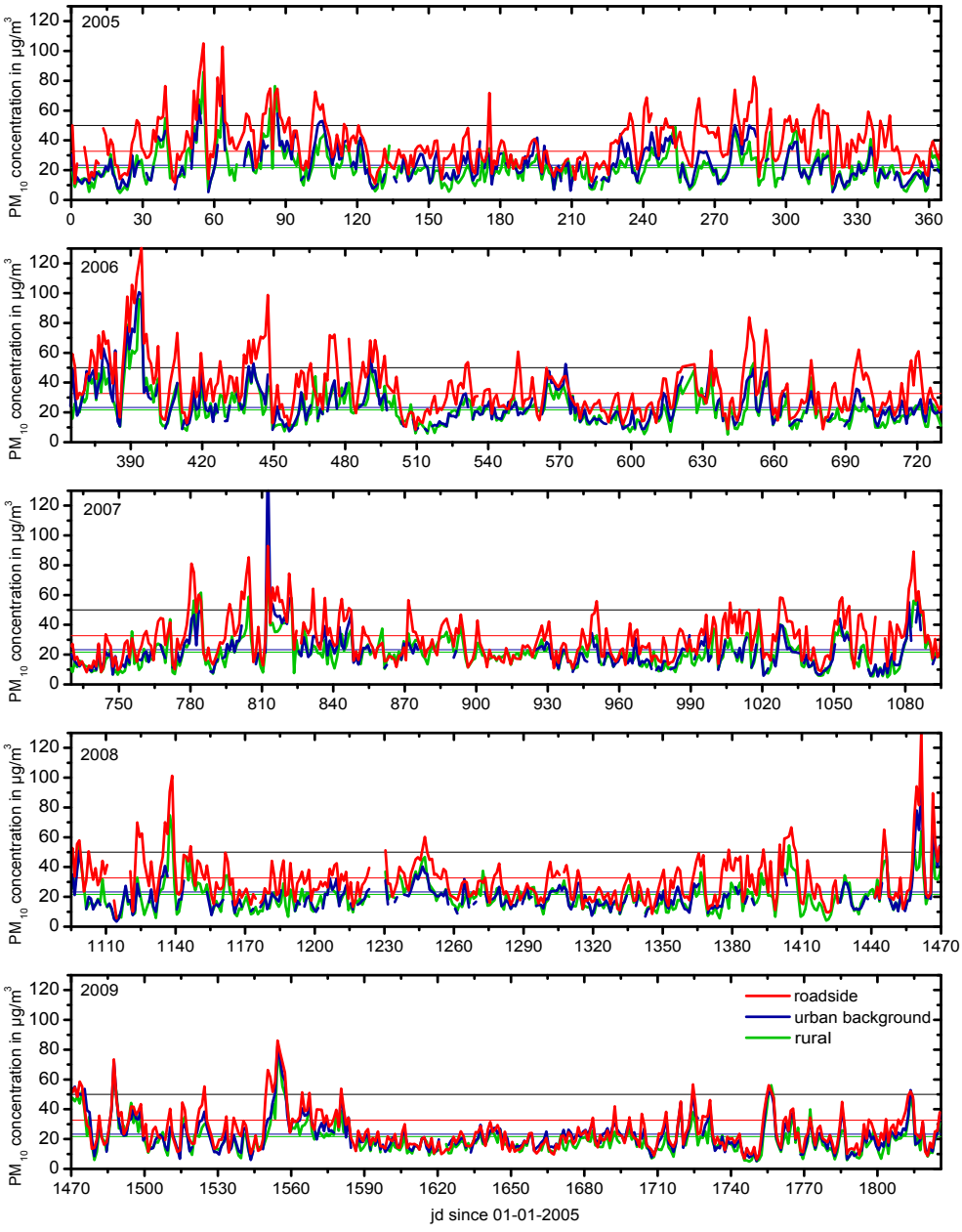

Fig. 2. Daily average PM_{10} concentrations at the three measurement sites (roadside, urban background, rural background) during 2005–2009. Colored lines indicate the average values over the entire period for each station; the black line displays the limit value of 50 µg m^{-3}.

$PM_{10} > 50\,\mu g\,m^{-3}$ at all sites (Fig. 2). These correspond to pollution episodes that tend to affect wide spatial areas.

Not unexpectedly, the mass concentrations at roadside were usually higher than or equal to those at the urban and rural background sites (Fig. 2). The difference between the averages of the urban and rural background concentrations was, however, found to be negligible within the measurement uncertainty.

This similarity of urban and rural background values suggests that diffuse urban sources seem to play only a minor role in Leipzig, at least in the residential area where the urban background site is situated (Leipzig-West). Local traffic sources appear to account for the major fraction of spatial variation in PM_{10}, which is supported by PM transport simulations on behalf of the municipal authorities (The City of Leipzig, 2009). As a conclusion, it does not matter greatly for this study whether the calculation of the roadside increment uses the urban background or rural background levels as a baseline.

Figure 3a compares roadside and rural background PM_{10} values for the period 2005–2009, yielding a general positive correlation with a slope of 1.43. As indicated by the

Table 1. Average PM_{10} and $PM_{2.5}$ particle mass concentrations over the five year period of this study (μ), in $\mu g\,m^{-3}$. The Table includes the standard deviations of the mean (σ_μ).

location	PM_{10}		$PM_{2.5}$	
	μ	σ_μ	μ	σ_μ
Leipzig-Mitte (roadside)	32.6	0.4	18.2	0.5
Leipzig-West (urban backgrund)	22.0	0.3		
Melpitz (rural background)	21.7	0.3	17.4	0.3

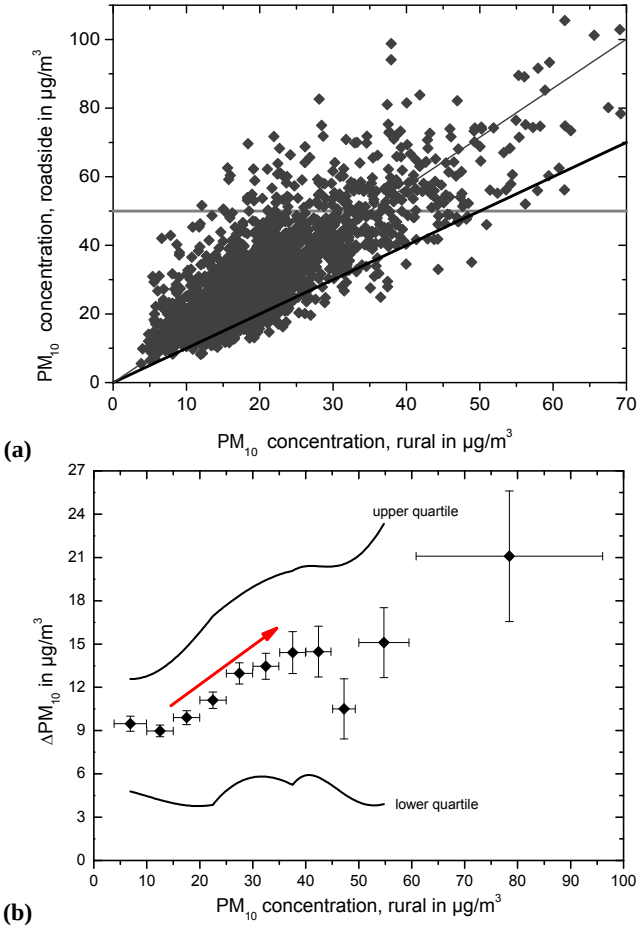

Fig. 3. Comparison between rural PM_{10}, roadside PM_{10} and the roadside increment ΔPM_{10}, 2005–2009. In **(a)** the daily limit value of $50\,\mu g\,m^{-3}$ is indicated by a horizontal line. A linear fit through the origin yields a slope of 1.43 ($R^2 = 0.62$). In **(b)** data were averaged over bins of rural PM_{10} indicated by x-axis whiskers. Y-axis whiskers indicate the standard error of the mean. The range of a multiplicative effect in the roadside increment ΔPM_{10} is indicated by a red arrow.

line of unity, the roadside values exceed the rural background concentrations in the overwhelming number of cases so that a meaningful roadside increment can be calculated. On individual days, the roadside increment could reach up to $60\,\mu g\,m^{-3}$.

Table 2. Number of exceedances per year of the daily limit value for PM_{10}. The number of valid measurement days is added in brackets.

year	Leipzig-Mitte roadside		Leipzig-West urban background		Melpitz rural background	
2005	70	(354)	9	(358)	8	(356)
2006	71	(348)	17	(350)	11	(350)
2007	38	(356)	6	(359)	10	(359)
2008	28	(337)	5	(337)	6	(353)
2009	25	(363)	18	(362)	11	(355)

Figure 3b takes a look into the relationship between rural background PM_{10} and the roadside increment ΔPM_{10}. For this purpose, ΔPM_{10} data were averaged over the bins of rural PM_{10} indicated by x-axis whiskers. Figure 3b indicates arithmetic mean values of ΔPM_{10}, with the standard deviation of the mean as a whisker. The central result is that ΔPM_{10} is ruled by a superposition of an additive effect around $9\,\mu g\,m^{-3}$, and a multiplicative effect (indicated by a red arrow). The multiplicative effect implies that ΔPM_{10} depends on the level of PM_{10} already present in the rural background. Concrete numbers suggest that between an average of rural PM_{10} of 10 and $40\,\mu g\,m^{-3}$, ΔPM_{10} amounts from 9.5 to $14.5\,\mu g\,m^{-3}$, i.e. by around $2.5\,\mu g\,m^{-3}$ per increase in $10\,\mu g\,m^{-3}$ increase in rural background.

4.2 Exceedances of the daily limit value

The availability of daily PM_{10} values at the roadside station was 1788 out of 1826 possible days, i.e. 98 %. These data were measured by the reference filter method.

On 232 of these 1788 days, the daily limit value of $50\,\mu g\,m^{-3}$ was exceeded. These 13 % of all days are called "exceedance days" in the following. Table 2 lists the number of daily limit value exceedances per year and site. At roadside, the Council Directive (no more than 35 exceedances/year) was violated in 2005, 2006 and 2007. The background stations featured consistently less than 35 exceedances per year, so we focus on the analysis of exceedance days at the roadside site hereafter. Since the urban and rural background average PM_{10} concentrations were very similar, we only used the rural site as a background measure in the following.

Figure 4 contrasts exceedance and non-excceedance days through their distribution of PM_{10} values. Figure 4a illustrates the rather trivial split of roadside concentrations into exceedance and non-exceedance days. A majority of exceedance days ($n = 207$) shows concentrations between 50 and $80\,\mu g\,m^{-3}$, while higher values up to the maximum of $130\,\mu g\,m^{-3}$ were scarcely found ($n = 25$). This highlights that the problem of limit value exceedances is essentially caused by a modest surplus of up to $30\,\mu g\,m^{-3}$ in PM_{10} at the roadside station.

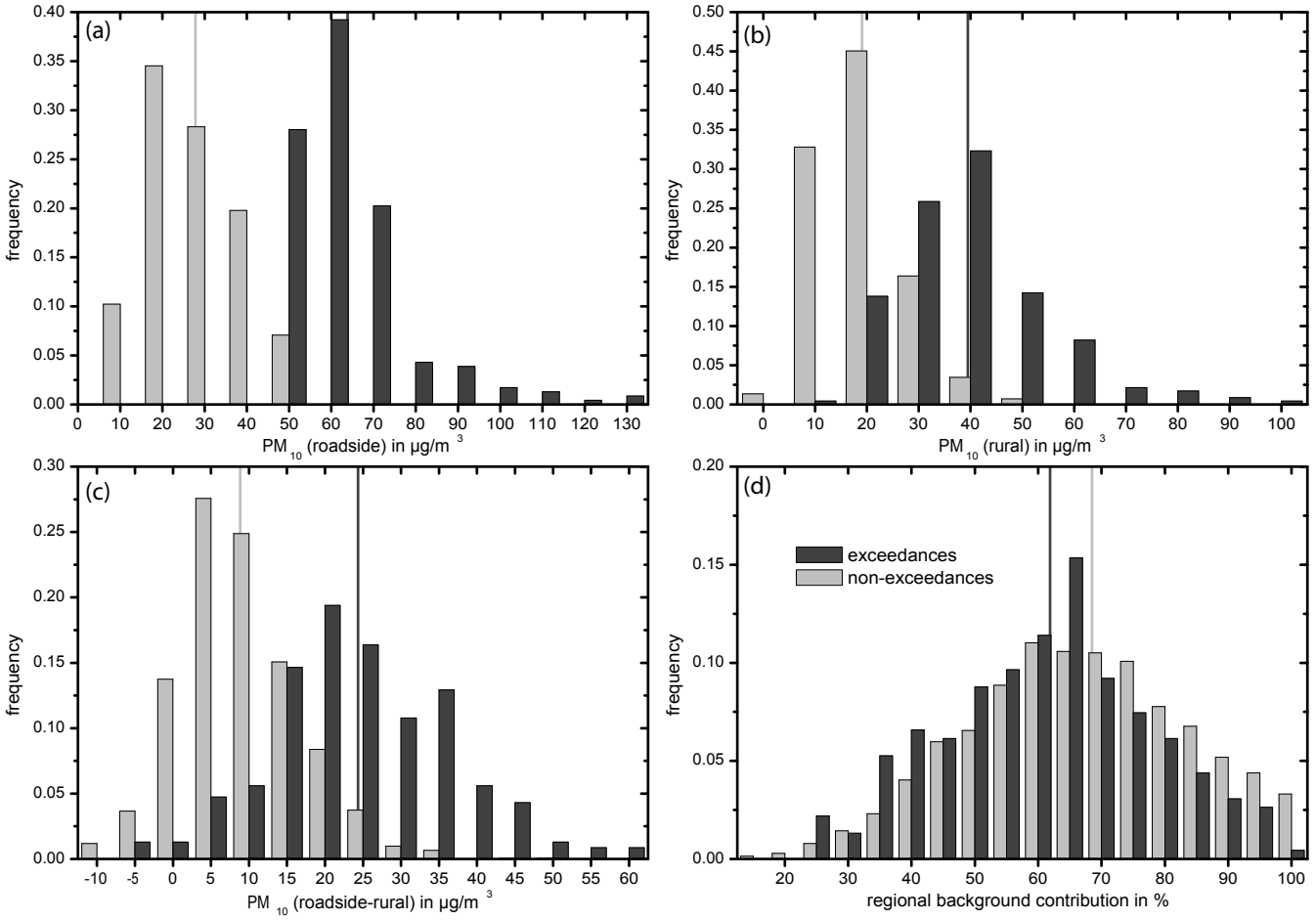

Fig. 4. Relative frequency distributions of **(a)** PM_{10} mass concentration at roadside, **(b)** PM_{10} mass concentration in the rural background, **(c)** the traffic contribution at roadside ($PM_{10,roadside}$–$PM_{10,rural}$), and **(d)** the regional background contribution at roadside ($PM_{10,rural}/PM_{10,roadside}$). The populations for exceedance and non-exceedance days were normalised separately. Vertical lines indicate the median values of each population.

In Fig. 4b the rural background concentrations show a different split, with partly overlapping populations: On non-exceedance days, PM_{10} was 19 µg m^{-3} on average. On exceedance days, PM_{10} amounted to 40 µg m^{-3} on average, which corresponds to 80 % of the daily limit value. On 46 days, the daily limit value was exceeded in the rural background atmosphere already. It is evident from Fig. 4b (though not surprising) that high PM_{10} in the rural background atmosphere increase the likelihood of a limit value exceedance at roadside.

The contribution of traffic to PM_{10} at roadside can be estimated by subtracting the corresponding rural background concentration, i.e. by calculating $PM_{10,roadside-rural}$ (ΔPM_{10}). Figure 4c demonstrates that this roadside increment can be highly variable: Between 0 and 35 µg m^{-3} (mean: 8 µg m^{-3}) on non-exceedance days, and between 5 and 65 µg m^{-3} (mean: 24 µg m^{-3}) on exceedance days. The roadside increment is clearly enhanced on exceedance days compared to non-exceedance days (mean values 24 vs. 8 µg m^{-3}), no less than the rural background concentrations (mean values 40 vs. 19 µg m^{-3}).

Figure 4d displays the relative contribution of the regional background to PM_{10} at roadside ($PM_{10,rural}/PM_{10,roadside}$). Importantly, the histograms for exceedance days compared to non-exceedance do not differ remarkably. On exceedance days, 62 % of the PM_{10} at roadside is assumed to originate from the regional background atmosphere, and 69 % on non-exceedance days. Importantly, the proportion between the contributions of regional sources and local traffic does not depend on whether a limit value exceedance occurred or not.

4.3 Seasonal effects

To better understand the PM_{10} exceedances, correlations with a variety of factors including season and local meteorological parameters were examined. Figure 5 shows the occurrence of the exceedance days as a function of the month of the year. Rather obviously, the exceedance days

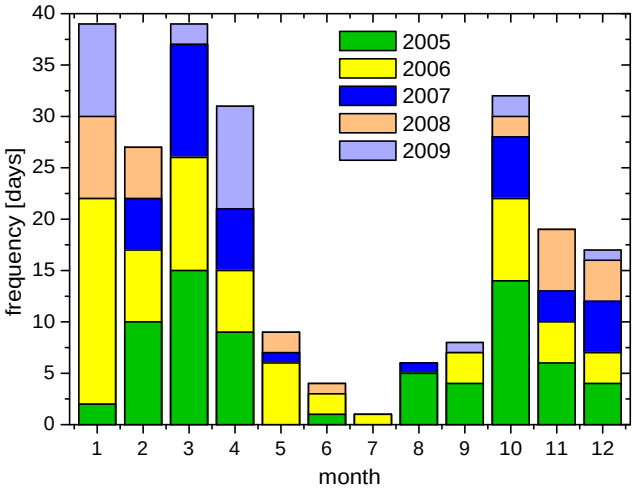

Fig. 5. Exceedances of the daily PM_{10} limit value at the roadside site Leipzig-Mitte keyed after month of the year. Data coverage: 2005-2009.

concentrate on the cold season (October to April), with rather few exceedances occurring during the summer months May-September. There are two general explanations for this imbalance: First, enhanced PM emissions from heating and power generation. Such emissions have been shown to lead to enhanced levels of PM_{10} in certain hotspots as well as in the rural background (Herrmann et al., 2006). Second, temperature inversions that lead to pollution trapping near the ground are more frequent during the cold season (e.g., Schäfer et al., 2006; Birmili et al., 2010).

In order to differentiate the influences of different particle source types, total PM_{10} as well as the coarse particle subfraction $PM_{[2.5;10]}$ are distinguished after season in Fig. 6. Note that the coarse fraction $PM_{[2.5;10]}$ was calculated as $PM_{10} - PM_{2.5}$.

The main findings from Fig. 6 can be summarised as follows:

(a) For exceedance days, PM_{10} shows a seasonality for both, roadside and rural background values, with the highest values occurring in winter and spring. This seasonality appears more pronounced in the rural background compared to roadside. On non-exceedance days, this seasonality is much less visible.

(b) $PM_{[2.5;10]}$ makes up a significant fraction of PM_{10}. At roadside, the relative fraction varies between 42% in winter and 49% in summer. $PM_{[2.5;10]}$ shows a seasonality different from PM_{10}, with maximum values in summer. This can usually be explained by increased resuspension rates in the dry summer months.

(c) Exceedance days feature a consistently higher roadside-to-rural ratio for PM_{10} as well as $PM_{[2.5;10]}$ in comparison to non-exceedance days. This highlights that an impact of local traffic sources is instrumental in generating exceedance days. The biggest roadside-to-rural ratios can be observed on exceedance days in summer. This means that in summer, when PM_{10} is generally lower, overproportional contributions from local traffic are required for PM_{10} to exceed the 50 µg m^{-3} threshold.

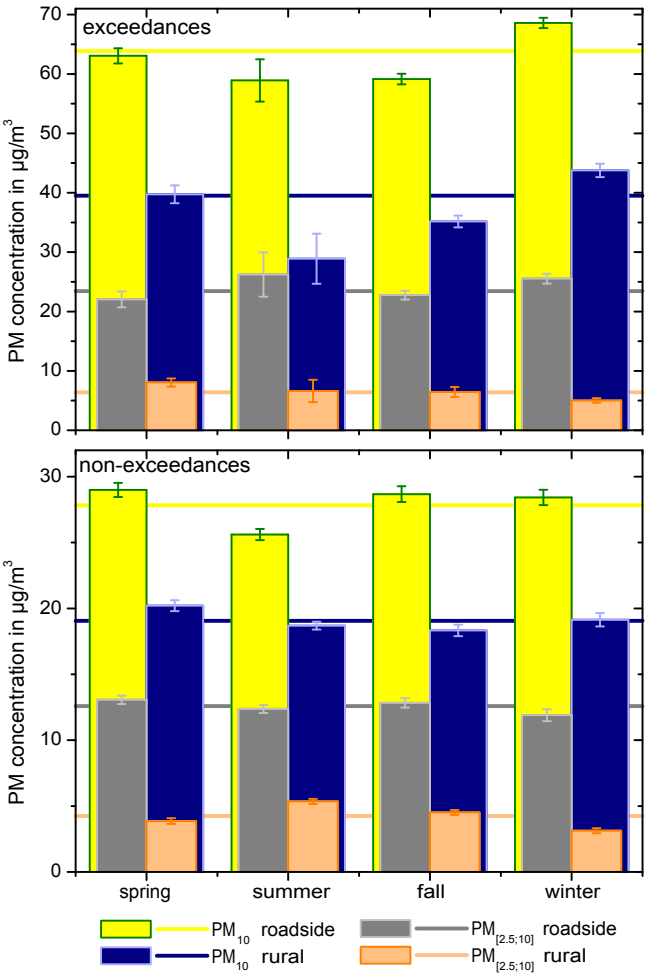

Fig. 6. Seasonal dependence of PM_{10} and $PM_{[2.5;10]}$ at roadside and in the rural background. The display distinguishes between exceedance days (upper graph) and non-exceedance days (lower graph). Horizontal lines indicate annual average values. The seasons were defined as winter (December–February), spring (March–May), summer (June–August), fall (September–November).

4.4 Chemical composition of rural background PM_{10}

We used data on the chemical composition of bulk PM_{10} to examine the particle sources that might be responsible for high PM concentrations. Long-term data on chemical particle composition has been available for the rural site Melpitz only.

Figure 7 shows that the bulk of PM_{10} is made up by ammonium nitrate, sulfate, as well as elemental and organic carbon.

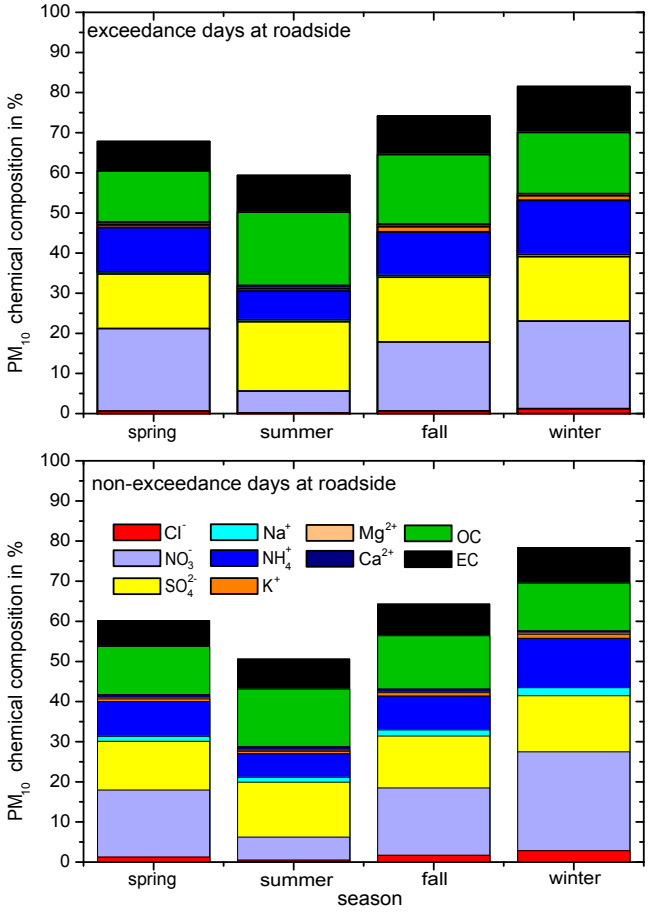

Fig. 7. Chemical mass fractions of rural background PM_{10} for each season and **(a)** exceedance days at roadside and **(b)** non-exceedance days at roadside. The gap between the total amounts shown and 100 % is material not accessible to the analytical procedures; this is interpreted as insoluble crustal material.

This is in broad agreement with most places in Western, Central and Northern Europe (Putaud et al., 2010).

The summer data reveals two peculiarities: First, nitrate is largely absent in PM_{10}, which is very likely due to the partitioning into the gas phase at high temperatures (Flechard and Fowler, 1998). Aerosol mass spectrometric measurements in Melpitz (Poulain et al., 2011) confirmed that the gas phase partitioning of nitrate is mainly a temperature-driven effect and does occur not only on a seasonal cycle but also on a diurnal cycle.

Second, the fraction of unidentified material is the highest in summer, 40 % on event days and 50 % on non-event days (Fig. 7). This material is associated with unsoluble crustal material that usually shows the highest emission rates during the dry summer period. The unidentified fraction is assumed to contain mainly silicates and insoluble carbonates, according to previous work, such as Espinosa et al. (2002). This assumption is supported by the slightly increased coarse particle mass concentration in summer (see Fig. 6). It is also consistent with the multi annual aerosol study in Augsburg, southern Germany (Birmili et al., 2010), which found a maximum of coarse particles in summer apparently originating from coarse particle resuspension.

The crucial result is that exceedance days are associated with an excess of EC, OC and ammonium sulphate, but with a deficiency of unidentified material, ammonium nitrate and sodium chloride. As EC, OC and ammonuim sulphate are typical tracers of anthropogenic emissions over the continent, we conclude that diffuse anthropogenic emissions play their role in raising the rural background PM levels and ultimately leading to PM_{10} exceedances at roadside. The highest EC and OC concentrations were found during winter exceedance days.

4.5 Meteorological influence

Table 3 contrasts exceedance and non-exceedance days with the aid of the local meteorological parameters and trace gas concentrations. Values in bold face indicate that the two subsets are significantly different on the basis of a Mann-Whitney-U-test (Wilcoxon, 1945; Mann and Whitney, 1947) with significance level $\alpha = 0.95$. The results for the various PM parameters are added for completeness, although the fact that the PM parameters are enhanced on exceedance days is rather intuitive, if not trivial.

Two main findings emerge from Table 3, which explain the occurrence of exceedance days in the cold, and warm seasons, respectively: In the cold season, mostly evident in the winter data, exceedance days are characterised by a combination of (a) low temperature, (b) high air pressure, (c) low wind speed, (d) low amount of precipitation, (e) enhanced concentrations of SO_2, NO and NO_2, and (f) reduced concentrations of O_3. On exceedance days, lower dew point temperatures and absolute humidities were found, but no significant correlation could be found with relative humidity.

These circumstances describe synoptic situations over Central Europe featuring high air pressure and slowly moving air masses. These situations have been described for the atmospheric aerosol by Birmili et al. (2001).

A surprising result is that the relative fraction of the roadside increment is not enhanced on those winter exceedance days. The PM_{10} roadside increment usually amounts to about 1/3 of the roadside concentration, and this fraction is practically invariable throughout the seasons of fall, winter and spring (Table 3). This implies a coupling of the average regional background and roadside increment concentrations, although the roadside increment itself can be highly variable in time (cf. Figure 3b). In other words this correlation implies that if the regional background concentration is high, the roadside increment also tends to be higher by a similar proportion. This finding shows that the effects of local and distant sources cannot be truly separated in their effect on the absolute roadside concentrations. Both contributions can therefore be regarded as equally responsible for exceedance

Table 3. Characteristics of exceedance days (left numbers, also indicated by n) compared to non-exeedance days (right numbers). Bold face indicates a significant difference in the Whitney-Mann-U test on the confidence level $\alpha = 0.95$. The tests were made for the total data set and all four seasons individually. Red face indicates significantly higher values, blue face significantly lower values. The temperature anomaly was calculated as the daily mean temperature minus the climatological average temperature for that day of the year.

parameter	unit	All ($n = 232$)	Spring ($n = 79$)	Summer ($n = 11$)	Fall ($n = 59$)	Winter ($n = 83$)
temperature	°C	**5.9**/11.1	8.7/10.3	**20.9**/18.7	10.2/10.6	**−1.9**/2.9
temperature anomaly	°C	**−0.5**/0.6	0.9/0.3	**3.6**/0.3	1.1/0.7	**−3.5**/1.2
dew point temperature	°C	**3.1**/7.7	**4.4**/6.2	**16.8**/13.6	8.1/8.1	**−3.8**/1.0
relative humidity	%	**82.3**/79.4	74.4/75.5	77.4/72.2	**86.9**/84.4	87.2/87.3
absolute humidity	g/kg	**5.9**/8	**6.4**/7.2	**14.1**/11.6	8.3/8.2	**3.7**/5.2
air pressure	hPa	**1011**/1006	**1008**/1003	1010/1007	**1011**/1008	**1015**/1006
wind speed	m/s	**1.5**/2.5	**1.5**/2.4	**1.1**/1.9	**1.5**/2.6	**1.5**/3.3
precipitation	mm/day	**0.2**/1.3	**0.2**/1.3	1.8/1.8	**0.1**/1.2	**0.1**/0.9
SO_2	$\mu g\,m^{-3}$	**5.0**/2.7	**4.5**/2.7	2.5/2.3	**3.4**/2.6	**6.8**/3.3
O_3	$\mu g\,m^{-3}$	**48**/61	72/70	87/79	**34**/46	**31**/45
NO_2	$\mu g\,m^{-3}$	**15.6**/9.1	**12.2**/8	**7.9**/6.5	**13.9**/10.2	**21.1**/12.4
NO	$\mu g\,m^{-3}$	**2.7**/1.4	**1.8**/1.3	1.1/1.2	**2.9**/1.4	**3.5**/1.6
PM_{10}						
roadside concentration	$\mu g\,m^{-3}$	**64***/28	**63***/29	**59***/26	**59***/29	**69***/28
urban background concentration	$\mu g\,m^{-3}$	**42**/19	**42**/20	**29**/19	**37**/19	**46**/19
rural background concentration	$\mu g\,m^{-3}$	**40**/19	**40**/20	**29**/19	**35**/18	**44**/19
roadside increment	$\mu g\,m^{-3}$	**24**/9	**23**/9	**30**/7	**24**/10	**25**/9
roadside increment	%	**35**/31	33/32	**51**/26	37/35	33/32
urban background increment	%	3/0	**4**/0	0/1	3/1	3/0
regional background	%	**62**/69	**63**/70	**49**/73	59/64	64/67
$PM_{2.5}$						
roadside concentration	$\mu g\,m^{-3}$	**38**/15	**40**/16	**31**/13	**36**/16	**37**/18
rural background concentration	$\mu g\,m^{-3}$	**33**/15	**31**/17	**22**/13	**29**/14	**39**/16
$PM_{[2.5;10]}$						
roadside concentration	$\mu g\,m^{-3}$	**23**/13	**22**/13	**26**/12	**23**/13	**26**/12
rural background concentration	$\mu g\,m^{-3}$	**6.4**/4.2	**8.0**/3.9	**6.6**/5.4	**6.5**/4.5	**5.0**/3.1
roadside increment	%	**38**/46	35/45	**46**/49	**39**/47	**41**/42
regional background	%	**17**/22	21/18	21/28	**19**/24	**11**/17

* trivial, because exceedance days are defined by $PM_{10} > 50\,\mu g\,m^{-3}$.

of the daily limit value. Reducing either of the two will help to improve the statistics of PM_{10} exceedances.

A clearly different mechanism applies to the relatively few exceedance days in summer ($n = 11$): Here, the roadside increment amounts to an unusually high value of 51 % compared to 26 % on non-exceedance days (Table 3). This highlights that exceedances in summer can only occur if there is an unusually high contribution by the local traffic sources. There are no indications that the coarse particle mode would contribute beyond its usual proportion to those summer exceedances. Those summer exceedance days seem rather accidental events that feature, at least, warmer temperatures and lower wind speeds than the usual conditions in summer.

5 Back trajectory cluster analysis

Back trajectory cluster analysis was performed to specify the potential influence of synoptic-scale meteorological conditions on the occurrence of PM_{10} exceedances. Figure 8 shows the results for a cluster analysis with $k = 9$ clusters, displaying the geographical origin of the air mass, the prevailing vertical stratification of the atmosphere as well as the absolute number of PM_{10} exceedances and the seasonal distribution of the measurement days within each cluster. In Fig. 8 the clusters were arranged according to the descending absolute number of PM_{10} exceedances.

5.1 Basic characteristics

The cluster analysis distinguishes between two major meteorological aspects: (a) air mass origin and vorticity of the flow, and (b) vertical stratification at noon time, which is climatologically linked to season. Clusters 1–4 share the common feature that their back trajectories originate from continental areas, and tend to be anticyclonic (Fig. 8a). More specifically, cluster 1 represents slowly moving air masses from southern Europe, cluster 2 air masses from Eastern Europe. Cluster 3

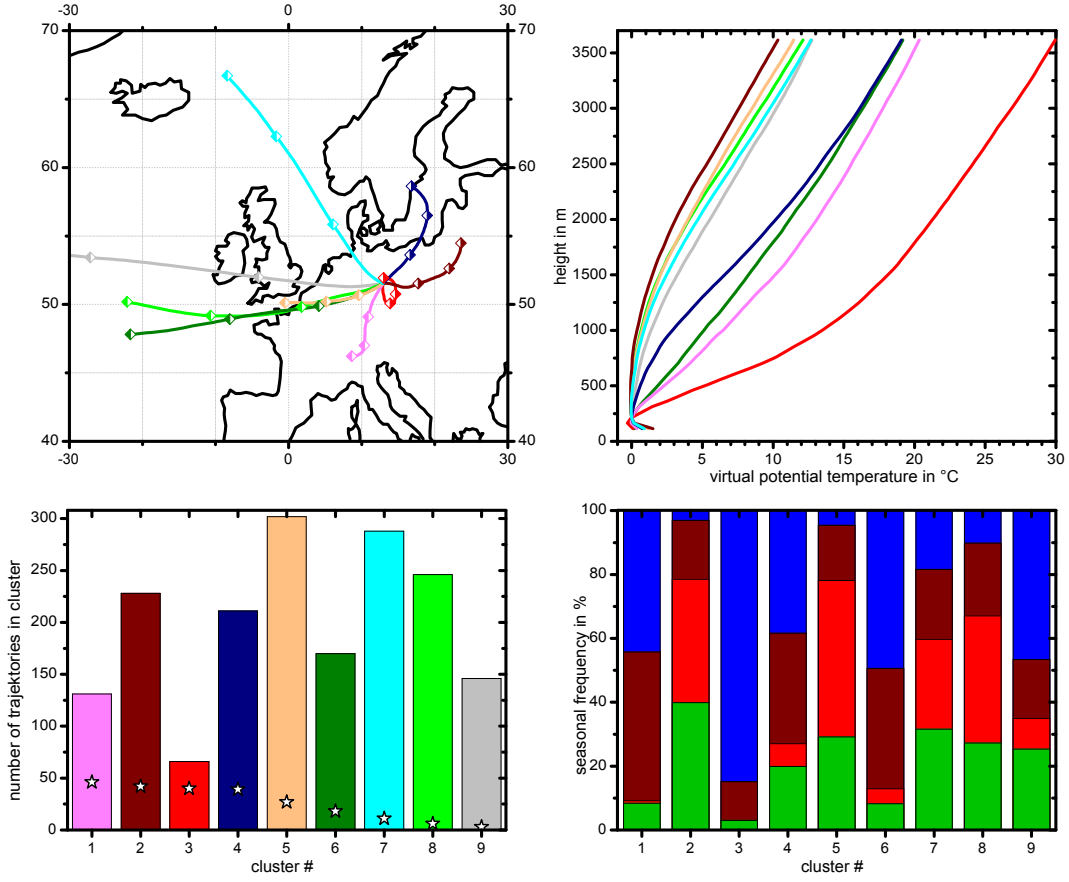

Fig. 8. Results of the back trajectory cluster analysis, 2005-2009: **(a)** mean back trajectories, **(b)** mean pseudo-potential temperature profiles, **(c)** frequency of the clusters in days (bars) including the number of limit value exceedances (star), **(d)** seasonal occurrence of each cluster (green: spring, red: summer, brown: fall, blue: winter).

represents stagnant air masses and cluster 4 air masses from Scandinavia. All other clusters (5–9) originate over the North Atlantic and tend to pass much shorter times over the continent.

The nine clusters can also be broken down into five clusters associated primarily with winter and autumn periods (1, 3, 4, 6, 9) and four clusters representing primarily spring and summer periods (2, 5, 7, 8) (Fig. 8d). This seasonality is also reflected in the vertical profiles of pseudo-potential temperature, typically showing temperature inversions at noon time in the cold season but neutral stratification (well-mixed conditions) for the warm season clusters (Fig. 8d).

5.2 PM levels

The nine clusters are sorted in descending order of their absolute number of PM_{10} exceedances at Leipzig-Mitte. 72 % of the PM_{10} exceedances are accounted for by the first four clusters (1–4) alone. The common feature of these clusters is that their three-day back trajectories originate over continental areas, and tend to be anticyclonic (Fig. 8).

Cluster 3 stands out in that it shows the highest PM_{10} values both in the background and at roadside (Fig. 9). In cluster 3, PM_{10} reaches an average rural background concentration of 40 $\mu g\,m^{-3}$. It is obviously a consequence that it also shows the highest probability of an exceedance to occur (61%, cf. Table 4). Cluster 3 is meteorologically characterised by stagnant air, the largest fraction of winter periods (85 %, Fig. 8d) and the most intense temperature inversions (Fig. 8b). These circumstances cover well the Central European air mass types denoted by “cP” or “cA” (Birmili et al., 2001).

Despite the extremely high PM_{10} values, cluster 3 represents a weather situation that occurs only rarely (4% of the time), so it ranks only third in the list of absolute number of exceedances.

For each of the clusters 1–6, one or several meteorological factors can be made responsible for the PM exceedances to occur: residence time of more than three days over the continent (1–5) and/or stable vertical stratification (1, 3, 4, 6). The probability of a PM exceedance to occur falls below 4 % only for the three last clusters (7–9) that show both, the Atlantic

Table 4. Frequency, mean meteorological parameters and trace gas concentrations for each cluster. Bold face indicates clusters where a particular parameter is significantly different from the overall population. Red face indicates significantly higher values, blue face significantly lower values. The temperature anomaly was calculated as the daily mean temperature minus the climatological average temperature for that day of the year. The season index is a number between −1 (corresponding to midwinter, 21 December) and +1 (midsummer, 21 June), giving an impression of the seasonal distribution of a particular cluster.

parameter/cluster	unit	mean	1	2	3	4	5	6	7	8	9
air mass			S	E	st.	NE	WSW	WSW	NW	WSW	W
season index			−0.46	0.43	-0.69	−0.12	0.44	−0.46	0.13	0.29	−0.23
frequency	%		7	13	4	12	17	9	16	14	8
exceedance days		232	46	42	40	39	27	18	11	6	3
probability of exceedance	%	13	35	18	61	18	9	11	4	2	2
temperature	°C	10.4	**5.8**	**16.1**	**−2.1**	**5.1**	**15.9**	**7.3**	**8.3**	**14.2**	**8.8**
temperature anomaly	°C	0.5	0.6	**1.9**	**−4.3**	**−1.8**	**1.5**	**2.3**	**−2.2**	**1.5**	**2.9**
dew point temperature	°C	7.1	**4.2**	**10.7**	**−4**	**3.0**	**11.8**	**5.1**	**5.0**	**10.2**	**5.5**
relative humidity	%	80	**90**	70	**87**	**86**	**76**	**86**	79	**77**	80
absolute humidity	g/kg	7.7	**6.4**	**9.6**	**3.6**	**5.9**	**10.4**	**6.8**	**6.7**	**9.4**	**6.9**
air pressure	hPa	1007	**1005**	1010	**1015**	**1012**	**1004**	1006	1007	**1005**	**1002**
wind speed	m/s	2.4	**2.0**	**1.7**	**1.8**	2.1	**1.7**	**2.8**	2.5	**2.9**	**4.3**
precipitation	mm/day	1.2	1.0	**0.8**	**0.1**	**0.6**	1.6	1.5	0.9	**1.9**	**1.5**
SO_2	$\mu g\,m^{-3}$	3	**3.6**	**3.2**	**8.0**	**3.5**	2.6	3.0	**2.1**	**2.4**	**2.1**
O_3	$\mu g\,m^{-3}$	59	**31**	**80**	**31**	**46**	**73**	**41**	59	**67**	60
NO_2	$\mu g\,m^{-3}$	10.0	**15.6**	**7.8**	**18.9**	**11.2**	9.2	**13.7**	**7.8**	**7.9**	**8.4**
NO	$\mu g\,m^{-3}$	1.6	**2.6**	1.4	**3.2**	**1.6**	1.6	**1.9**	**1.1**	**1.1**	**1.0**
PM_{10}											
roadside concentration	$\mu g\,m^{-3}$	32.6	**45.7**	38.8	**56.7**	**37.3**	32.8	31.5	**26.2**	**23.4**	**22.9**
urban background concentration	$\mu g\,m^{-3}$	22.0	**31.1**	**30.2**	**46.2**	**25.8**	**23.6**	**20.5**	**16.2**	**17.4**	**14.9**
rural background concentration	$\mu g\,m^{-3}$	21.7	**31**	**27**	**40.5**	**24.5**	**22.1**	20.0	**15.1**	**17.1**	**14.0**
roadside increment	$\mu g\,m^{-3}$	11.2	**14.6**	**11.9**	**16.2**	**13.3**	11.1	11.6	11.1	**6.7**	**9.2**
roadside increment	%	29	32	**22**	**18**	31	28	**35**	**38**	**26**	35
urban background increment	%	4.9	**0.2**	8.3	10	3.4	4.5	1.7	4	1.5	**4**
regional background	%	66	68	**70**	**72**	66	67	63	**58**	**73**	**61**
$PM_{2.5}$											
roadside concentration	$\mu g\,m^{-3}$	18.2	**28.1**	**21.6**	**33.1**	**23.7**	20.3	16.7	**11.0**	**12.6**	**10.6**
rural background concentration	$\mu g\,m^{-3}$	17.4	**26.6**	**21.0**	**36.0**	**20.2**	16.8	16.0	**11.5**	**12.8**	**9.9**
$PM_{[2.5;10]}$											
roadside concentration	$\mu g\,m^{-3}$	13.6	15.1	**16.6**	10.0	13.6	15.4	12.6	12.7	**10.4**	12.6
rural background concentration	$\mu g\,m^{-3}$	4.6	4.6	**6.1**	4.5	4.4	**5.3**	**4.1**	**3.8**	4.5	4.1
roadside increment	%	42	**33**	43	**18**	**36**	47	40	**49**	45	**55**
regional background	%	21	**15**	22	**12**	**18**	**23**	**19**	**23**	**26**	**27**

as a source region (Fig. 8a), wind speeds above $2.5\,m\,s^{-1}$, and neutrally stable stratification (Fig. 8b). The clusters 7–9 account for 38 % of the observation time but only for 8 % of the PM_{10} exceedances (Table 4).

5.3 Relationship to meteorology and gas phase species

Table 4 summarizes the properties of the nine clusters including average values of meteorological parameters, trace gases and PM parameters. As in the previous section, Mann-Whitney-U-tests were performed to check whether a cluster deviates from the overall mean with respect to the meteorological, trace gas and PM observations. Bold face in Table 4 indicates statistically relevant differences, with tendency being indicated by colour.

Temperature seems an instrumental factor for cluster 3, which represents average temperatures of −2.1 °C and a temperature anomaly of −4.3 °C. Over the continent, such deep temperatures lead to the formation of the temperature inversions depicted in Fig. 8b. At such temperatures, enhanced emissions from power generation and domestic heating are expected. It is likely that these factors contribute to the extreme PM concentrations of $40\,\mu g\,m^{-3}$ in the rural background.

Three out of the first clusters (1, 3, 4) are also characterised by an absolute humidity content below average (Table 4).

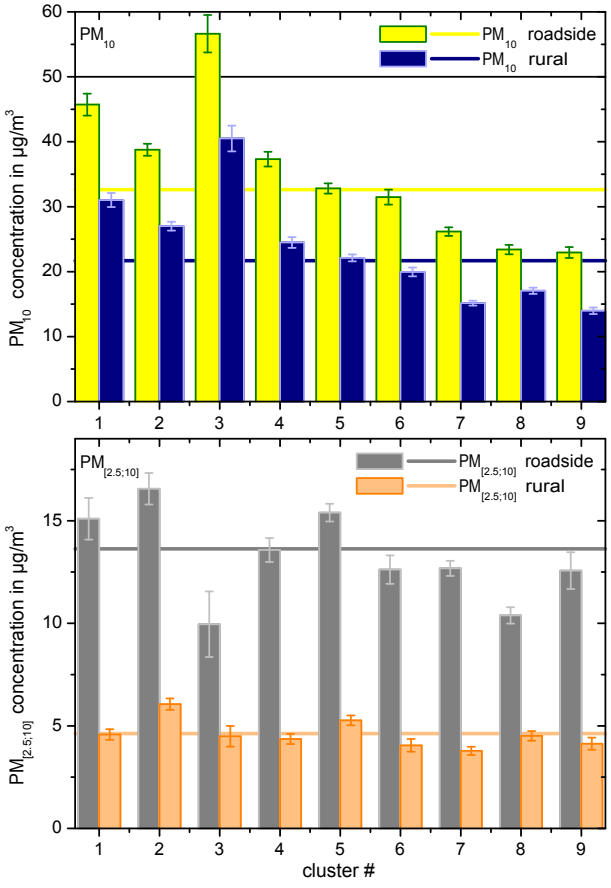

Fig. 9. PM_{10} and $PM_{[2.5;10]}$ concentration at roadside and regional background as well as standard deviation for each cluster. Horizontal lines indicate overall averages for a particular parameter.

This is likely due to the continental history of the air masses and generally leads to low amounts of precipitation, which is confirmed in the Table as well.

The first five clusters (1–5) show wind speeds on or below average (Table 4). This confirms that the poor dispersion conditions associated with these low wind speeds are a likely factor contributing to the PM exceedances. Air pressure is an indicator insofar as the clusters 3 and 4 are associated with high pressure areas residing over, or just north of Central Europe (Table 4).

Cluster 2 is a different case in that it shows a non-negligible fraction of exceedances (18 %), but represents warm conditions with good vertical mixing (Fig. 8b). While its trajectory indicates source regions over Eastern Europe (Fig. 8a), we also see some excess in coarse PM both at roadside and in the rural background (Fig. 9b). It can be thought that the rather warm and sunny conditions (as indicated by the ozone level of 80 µg m^{-3}) lead to the resuspension of coarse PM over dried-out surfaces. As indicated by the coarse PM data in Fig. 9b this resuspension seems to occur both, regionally and locally.

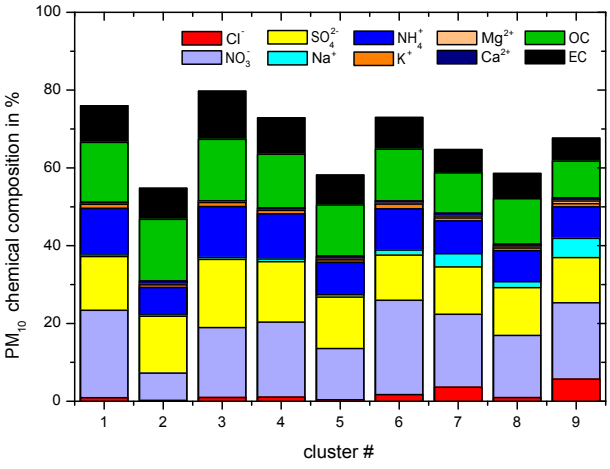

Fig. 10. Chemical composition of PM_{10} in the rural background during each cluster. The amount missing to 100% is inaccessible to the chemical analyses performed and interpreted as insoluble crustal material.

As another finding, the cold season clusters 1, 3 and 4 show a significant correlation with gas phase pollutants like SO_2 and NO_2 (Table 4). Especially SO_2 can be regarded as an indicator for regional pollution emissions and remote transport from distant source regions. Not surprisingly the peak pollution concentrations were found in the winter time cluster 3 described above.

5.4 Chemical composition of background PM

The chemical composition of PM_{10} at the rural background site Melpitz strongly depends on the air mass origin (Fig. 10).

Nitrate is scarce in clusters 2, 5, and 8, i.e. clusters associated with warm periods. As in Sect. 4.4, we explain this by the thermodynamic partitioning of nitrate into the gas phase. Nitrate is most abundant in cluster 6 (almost 25 % of the mass), i.e. air slowly moving towards our region under study from westerly wind directions. Sulphate is present in all clusters, but most abundant in cluster 3, which has been identified as stagnant inversion situation in wintertime above.

The clusters leading to most of the PM exceedances are characterised by an excess in carbonaceous species, OC and EC. EC amounts to roughly 10 % in cluster 3. As EC and OC are predominantly emitted and/or generated over land, we take these values as further evidence for the role of land-based emissions in generating a regional background of PM_{10}.

Chloride is only available in traces, but shows a clear relationship to high wind speeds and maritime source regions (clusters 7 and 9; Fig. 10). As the relative amounts of chloride in PM_{10} are inversely related to the number of PM exceedances, we conclude that sea salt plays no role for such exceedances in Leipzig.

Most variation, however, is included in the amount of PM inaccessible to chemical analysis. This unidentified mass fraction amounts to almost 50 % in some clusters. It is intriguing that this fraction is the highest in the warm season clusters 2, 5, and 8. This leads to the consistent picture that crustal material, which is assumed to be the major constituent in the unidentified fraction, is more abundant in the warm and dry season.

For cluster 2, the chemically unidentified fraction amounts to 17.5 $\mu g\,m^{-3}$. Meanwhile, the coarse PM mass concentration (in the size range 2.5–10 µm) amounts to 16.6 $\mu g\,m^{-3}$. The similarity of these values suggest a leading role of the diffuse resuspension source for the budget of PM_{10} in cluster 2. A roadside increment of coarse PM of 10.5 $\mu g\,m^{-3}$ highlights the relevance of resuspension due to local traffic for the PM_{10} exceedances in Leipzig.

6 Discussion

6.1 Local vs. regional contributions

Comparing the PM_{10} levels at roadside and in the rural background yields a positive trend across the nine trajectory clusters (Fig. 9). The relative contribution of local traffic-related sources was the highest for low background concentrations; nevertheless, the regional contribution was between 58 and 73 % of the local PM_{10} mass concentration. This is in good agreement with the results by Lenschow et al. (2001) in the city of Berlin, who found 50 % of urban PM_{10} originating from the regional background. They reported the traffic as the most important group of sources causing high PM_{10} concentrations at kerbside, with up to 15 % of PM_{10} mass concentration resulting from resuspended soil. These contributions show that horizontal advection of a regionally polluted air mass is usually not sufficient to cause an exceedance day at the traffic site.

However, the source contributions from regional, urban background and traffic related sources were surprisingly similar for all clusters, independent of the weather situation. This is why we suppose, that both regionally and locally close to ground emitted particles are accumulated in the boundary layer in case of favorable meteorological conditions, but the source contributions remain nevertheless similar. This would result in different absolute concentrations but the same relative contributions. To investigate this more detailed, the chemical composition has to be considered as well, which is displayed in Fig. 10 for the regional background site.

6.2 Analogies in Europe

Former studies have shown that the residence of air masses over continents leads to the accumulation of tropospheric aerosol. One reason is the presence of natural and anthropogenic sources over land. Another is the loss of moisture in air masses over land, which leads to a lesser degree of wet deposition in air masses that have travelled long over continents. Inversion situations and a low mixing layer height have, for example, been related to high concentrations of gases and particulates in other European (Kukkonen et al., 2005) or German cities (Schäfer et al., 2006).

Measurements in the United Kindgom have shown that the advection of air masses from continental Europe and the regional formation of secondary aerosol were responsible for the majority of exceedance days (Charron et al., 2007). These authors also found an increased regional background contribution for exceedance days.

Nitrate was identified as the leading chemical compound in PM_{10} during limit value exceedances (Yin and Harrison, 2008). These authors also found contributions of up to 40 % at kerbside. In this study, in comparison, more modest contributions of about 20 % were found for exceedance days, but nevertheless this secondary source was a main contributor to PM_{10} mass concentration as well.

In Spain, a comparable number of exceedance days was found by Escudero et al. (2007), but the reasons were seldom identified in continental air masses. In southern Europe, dust originating from resuspension over arid surfaces as well as remote transport of Saharan dust apparently play a crucial role in the generation of PM exceedances. Nevertheless, anticyclonic conditions in wintertime seem to cause an accumulation of regional pollution even over the Iberian peninsula.

In addition, Viana et al. (2007), identified significant episodes of PM_{10} pollution in western Europe with air masses of European origin. They concluded the origin of the exceedances being anthropogenic, but may be long-range transport and not only local pollution. As a matter of fact, trajectories from eastern Europe frequently coincide with anticyclonic scenarios, leading to air mass stagnation.

6.3 Future perspectives

In Germany, the national emissions for PM_{10} are expected to further decrease (updated information from UBA (2009)). However, this continuing trend of decreasing emissions has not yet been observed in the air quality networks. It therefore remains to be answered whether the emissions known to the air quality authorities correspond to the real emissions.

The year 2011 saw the introduction of a “low-emission-zone” in the city of Leipzig. This can be seen as a local governmental effort to reduce PM_{10} in the city. The low-emission-zone implies that only vehicles adhering to enhanced emission standards (Euro 4 and better) are permitted to enter the city. It is expected that this measure will reduce the local contributions to PM_{10}, including the toxicologically relevant substances relevant to diesel soot.

However, since the majority of traffic-related PM_{10} emissions are associated with abrasion and resuspension (Harrison et al., 2008), it is unclear whether the PM_{10} reductions will be sufficient to prevent future violations of the legal limit value. Dijkema et al. (2008) reported a more effective

reduction of PM_{10} at roadside due to speed limit reduction (and thus less resuspended road dust) compared to the impact of reduced emission vehicles. However, the non-exhaust-related traffic emissions, which increase with increasing traffic volume independent of exhaust emission regulations, are of environmental significance, since they may contain trace metals causing negative health effects as well (Weckwerth, 2001; Sternbeck et al., 2002). These non-exhaust emissions are more or less constant during the year but depending on the traffic volume, the type of road, the pavement and the meteorological conditions. They are reduced by rainfall of at least $2\,mm\,h^{-1}$, probably because this results in a relatively long period with wet road surface and thus reduced resuspension (Keuken et al., 2010).

7 Conclusions

Five years of PM_{10} and $PM_{2.5}$ measurements at three observation sites (roadside, urban and regional) were analyzed with respect to limit exceedances of PM_{10} according to the EC directive 1999/30/EC. Four specific weather situations have been recognized as favourable for limit exceedances in Leipzig. Each of them contributes about 18 % to the number of daily limit exceedances, thus explaining 72 % of the total number of exceedances. This indicates the complexity of the causes of limit value exceedances, and also the difficulty to predict such limit value exceedances by models.

Statistical and back trajectory cluster analysis yielded the result that PM_{10} concentrations were enhanced on a regional scale during specific wintertime weather situations: high pressure, low temperatures, lack of precipitation, low wind speeds and and stable stratification. Atmospheric stratification seemed instrumental in generating exceptionally high PM_{10} mass concentrations at roadside as well as in the regional background through accumulation below the atmospheric inversion. The coarse PM fraction at the roadside site was clearly higher than at the regional site. This points to the relevance of coarse particle emissions due to local traffic, likely caused by resuspension of road dust, break and tire abrasion.

Our analysis suggests that local as well as regional sources of PM are – in case of favourable meteorological conditions – equally responsible for exceedances days at the roadside site. The meteorological conditions can be critical in limiting dilution and thus in enhancing accumulation of the particles and thus influence the generation of exceedances. The conclusion is that a combined effort of local, national and international reduction measures appears most likely to avoid systematic exceedances of the daily limit value in the future.

Acknowledgements. C. E. acknowledges personal funding by the scholarship programm of the German Federal Environmental Foundation (DBU). We acknowledge the Saxon State Office for Environment, Agriculture and Geology, particularly Annette Pausch, for providing the PM_{10} and $PM_{2.5}$ data for Leipzig-Mitte and Leipzig-West.

Edited by: V.-M. Kerminen

References

Abdalmogith, S. and Harrison, R.: The use of trajectory cluster analysis to examine the long-range transport of secondary inorganic aerosol in the UK, Atmos. Environ., 39, 6686–6695, 2005.

Amato, F., Pandolfi, M., Escrig, A., Querol, X., Alastuey, A., Pey, J., Perez, N., and Hopke, P.: Quantifying road dust resuspension in urban environment by Multilinear Engine: A comparison with PMF2, Atmos. Environ., 43, 2770–2780, 2009.

Annesi-Maesano, I., Forastiere, F., Kunzli, N., and Brunekref, B.: Particulate matter, science and EU policy, Eur. Respir. J., 29, 428–431, 2007.

Baker, J.: A cluster analysis of long range air transport pathways and associated pollutant concentrations within the UK, Atmos. Environ., 44, 563–571, 2010.

Barmpadimos, I., Hueglin, C., Keller, J., Henne, S., and Prévôt, A. S. H.: Influence of meteorology on PM_{10} trends and variability in Switzerland from 1991 to 2008, Atmos. Chem. Phys., 11, 1813–1835, doi:10.5194/acp-11-1813-2011, 2011.

Beddows, D., Dall'Osto, M., and Harrison, R.: Cluster Analysis of rural, urban, and curbside atmospheric particle size data, Atmos. Environ., 43, 4694–4700, 2009.

Birmili, W., Wiedensohler, A., Heintzenberg, J., and Lehmann, K.: Atmospheric particle number size distribution in central Europe: Statistical relations to air masses and meteorology, J. Geophys. Res., 106, 32005–32018, doi:10.1029/2000JD000220, 2001.

Birmili, W., Schepanski, K., Ansmann, A., Spindler, G., Tegen, I., Wehner, B., Nowak, A., Reimer, E., Mattis, I., Müller, K., Brüggemann, E., Gnauk, T., Herrmann, H., Wiedensohler, A., Althausen, D., Schladitz, A., Tuch, T., and Löschau, G.: A case of extreme particulate matter concentrations over Central Europe caused by dust emitted over the southern Ukraine, Atmos. Chem. Phys., 8, 997–1016, doi:10.5194/acp-8-997-2008, 2008.

Birmili, W., Weinhold, K., Nordmann, S., Wiedensohler, A., Spindler, G., Müller, K., Herrmann, H., Gnauk, T., Pitz, M., Cyrys, J., Flentje, H., Nickel, C., Kuhlbusch, T., Löschau, G., Haase, D., Meinhardt, F., Schwerin, A., Ries, L., and Wirtz, K.: Atmospheric aerosol measurements in the German Ultrafine Aerosol Network (GUAN) Part 1: Soot and particle number size distributions, Gefahrst. Reinhalt. L., 69, 137–145, 2009.

Birmili, W., Heinke, K., Pitz, M., Matschullat, J., Wiedensohler, A., Cyrys, J., Wichmann, H.-E., and Peters, A.: Particle number size distributions in urban air before and after volatilisation, Atmos. Chem. Phys., 10, 4643–4660, doi:10.5194/acp-10-4643-2010, 2010.

Brankov, E., Rao, S., and Porter, P.: A trajectory-clustering-correlation methodology for examining the long-range transport of air pollutants, Atmos. Environ., 32, 1525–1534, 1998.

Bruckmann, P., Birmili, W., Straub, W., Pitz, M., Gladtke, D., Pfeffer, U., Hebbinghaus, H., Wurzler, S., and Olschewski, A.: An

Outbreak of Saharan dust causing high PM_{10} levels north of the Alps, Gefahrst. Reinhalt. L., 68, 490–498, 2008.

Brüggemann, E., Gnauk, T., Mertes, S., Acker, K., Auel, R., Wieprecht, W.,Müller, D., jr., J. C., Chang, H., Galgon, D., Chemnitzer, R., Rüd, C., Junek, R., Wiedensohler, A., and Herrmann, H.: Schmücke hill cap cloud and valley stations aerosol characterisation during FEBUKO (I): Particle size distribution, mass, and main components, Atmos. Environ., 39, 4291–4303, 2005.

Buchanan, C., Beverland, I., and Heal, M.: The influence of weather-type and long-range transport on airborne particle concentrations in Edinburgh, UK, Atmos. Environ., 36, 5343–5354, 2002.

Cape, J., Methven, J., and Hudson, L.: The use of trajectory cluster analysis to interpret trace gas measurements at Mace Head, Ireland, Atmos. Environ., 34, 3651–3663, 2000.

Charron, A., Harrison, R., Moorcroft, S., and Booker, J.: Quantitative interpretation of divergence between PM_{10} and $PM_{2.5}$ mass measurement by TEOM and gravimetric (Partisol) instruments, Atmos. Environ., 38, 415–423, 2004.

Charron, A., Harris, R., and Quincey, P.: What are the sources and conditions responsible for exceedances of the 24h PM_{10} limit value ($50\,\mu g\,m^{-3}$) at a heavily trafficked London site?, Atmos. Environ., 41, 1960–1975, 2007.

Dijkema, M., van der Zee, S., Brunekreef, B., and van Strien, R.: Air quality effects of an urban highway speed limit reduction, Atmos. Environ., 42, 9098–9105, 2008.

Dorling, S. R., Davies, T. D., and Pierce, C. E.: Cluster analysis: a technique for estimating the synoptic meteorological controls on air and precipitation chemistry – method and applications, Atmos. Environ., 26A, 2575–2581, 1992.

Draxler, R. R. and Hess, G. D.: Description of the HYSPLIT4 modeling system, NOAA Tech. Memo., ERL, ARL-224, 2004.

Dutkiewicz, V., Qureshi, S., Khan, A., Ferraro, V., Schwab, J., Demerjian, K., and Husain, L.: Sources of fine particulate sulfate in New York, Atmos. Environ., 38, 3179–3189, 2004.

EC(1996): Council directive 96/62/EC of 27 September 1996 on ambient air quality assessment and management, Official Journal of the European Communities, 1999.

EC(1999): Council directive 1999/30/EC of 22 April 1999 relating to limit values for sulfur dioxide, nitrogen dioxide and oxides of nitrogen, particulate matter and lead in ambient air, Official Journal of the European Communities, 1999.

Engler, C., Rose, D., Wehner, B., Wiedensohler, A., Brüggemann, E., Gnauk, T., Spindler, G., Tuch, T., and Birmili, W.: Size distributions of non-volatile particle residuals ($D_p < 800\,nm$) at a rural site in Germany and relation to air mass origin, Atmos. Chem. Phys., 7, 5785–5802, doi:10.5194/acp-7-5785-2007, 2007.

Escudero, M., Querol, X., Ávila, A., and Cuevas, E.: origin of the exceedances of the European daily PM limit value in regional background areas of Spain, Atmos. Environ., 41, 730–744, 2007.

Espinosa, A., Rodriguez, M., de la Rosa, F., and Sanchez, J.: A chemical speciation of trace metals for fine urban particles, Atmos. Environ., 36, 773–780, 2002.

Flechard, C. and Fowler, D.: Atmospheric ammonia at a moorland site. I: The meteorological control of ambient ammonia concentrations and the influence of local sources, Q. J. Roy. Meteor. Soc., 124, 733–757, 1998.

Gnauk, T., Brüggemann, E., Müller, K., Chemnitzer, R., Rüd, C., et al.: Aerosol characterisation at the FEBUKO upwind station Goldlauter (I): Particle mass, main ionic components,OCEC, and mass closure, Atmos. Environ., 39, 4209–4218, 2005.

Harrison, R., Stedman, J., and Derwent, D.: New Directions: Why are PM_{10} concentrations in Europe not falling?, Atmos. Environ., 42, 603–606, 2008.

Herrmann, H., Brüggemann, E., Franck, U., Gnauk, T., Löschau, G., Müller, K., Plewka, A., and Spindler, G.: A source study of PM in Saxony by size-segregated characterisation, J. Atmos. Chem., 55, 103–130, 2006.

Kemp, K.: A multipoint receptor model for long-range transport over southern Scandinavia, Atmos. Environ., 27, 823–830, 1993.

Keuken, M., van der Gon, H., and van der Valk, K.: Non-exhaust emissions of PM and the efficiency of emission reduction by road sweeping and washing in the Netherlands, Sci. Total Environ., 408, 4591–4599, 2010.

Kittelson, D. B.: Engines and nanoparticles: a review, J. Aerosol Sci., 29, 575–588, 1998.

Kukkonen, J., Pohjola, M., Sokhi, R., Luhana, L., Kitwiroon, N., Fragkou, L., Rantamäki, M., Berge, E., Ødegaard, V., Slørdal, L., Denby, B., and Finardi, S.: Analysis and evaluation of selected local-scale PM_{10} air pollution episodes in four European cities: Helsinki, London, Milan and Oslo, Atmos. Environ., 39, 2759–2773, 2005.

Lenschow, P., Abraham, H.-J., Kutzner, K., Lutz, M., Preuß, J., and Reichenbacher, W.: Some ideas about the sources of PM_{10}, Atmos. Environ., 35, 23–33, 2001.

Mann, H. and Whitney, D.: On a test of whether one of two random variables is stochastically larger than the other, Ann. Math. Stat., 18, 50–60, 1947.

Moody, J. and Galloway, J.: Quantifying the relationship between atmospheric transport and the chemical composition of precipitation on Bermuda, Tellus B, 40, 463–479, 1988.

Mukai, H. and Suzuki, M.: Using air trajectories to analyze the seasonal variation of aerosols transported to the Oki Islands, Atmos. Environ., 30, 3917–3934, 1996.

Neusüß, C., Pelzing, M., Plewka, A., and Herrmann, H.: A new analytical approach for size-resolved speciation of organic compounds in atmospheric particles: Methods and first results, J. Geophys. Res.-Atmos., 105, 4513–4527, 2000.

Pio, C. and Lopes, D.: Chlorine loss from marine aerosol in a coastal atmosphere, J. Geophys. Res.-Atmos., 103, 25263–25272, 1998.

Poulain, L., Spindler, G., Birmili, W., Plass-Dülmer, C., Wiedensohler, A., and Herrmann, H.: Seasonal and diurnal variations of particulate nitrate and organic matter at the IfT research station Melpitz, Atmos. Chem. Phys., 11, 12579-12599, doi:10.5194/acp-11-12579-2011, 2011.

Putaud, J.-P., van Dingenen, R., Alastuey, A., Bauer, H., Birmili, W., Cyrys, J., Flentje, H., Fuzzi, S., Gehrig, R., Hansson, H., Harrison, R., Herrmann, H., Hitzenberger, R., Hüglin, C., Jones, A., Kasper-Giebl, A., Kiss, G., Kousa, A., Kuhlbusch, T., Löschau, G., Maenhaut, W., Molnar, A., Moreno, T., Pekkanen, J., Perrino, C., Pitz, M., Puxbaum, H., Querol, X., Rodriguez, S., Salma, I., Schwarz, J., Smolik, J., Schneider, J., Spindler, G., ten Brink, H., Tursic, J., Viana, M., Wiedensohler, A., and Raes, F.: A European aerosol phenomenology – 3: Physical and chemical characteristics of particulate matter from 60 rural, urban, and kerbside sites across Europe, Atmos. Environ., 44, 1308–1320, 2010.

Querol, X., Alastuey, A., Ruiz, C., Artiñano, B., Hansson, H., Harrison, R., Buringh, E., ten Brink, H., Lutz, M., Bruckmann, P., Straehl, P., and Schneider, J.: Speciation and origin of PM_{10} and $PM_{2.5}$ in selected European cities, Atmos. Environ., 38, 6547–6555, 2004.

Rose, D., Wehner, B., Ketzel, M., Engler, C., Voigtländer, J., Tuch, T., and Wiedensohler, A.: Atmospheric number size distributions of soot particles and estimation of emission factors, Atmos. Chem. Phys., 6, 1021–1031, doi:10.5194/acp-6-1021-2006, 2006.

Sanders, P., Xu, N., Dalka, T., and Maricq, M.: Airborne Brake Wear Debris: Size Distributions, Composition, and a Comparison of Dynamometer and Vehicle Tests, Environ. Sci. Technol., 37, 4060–4069, 2003.

Schäfer, K., Emeis, S., Hoffmann, H., and Jahn, C.: Influence of mixing layer height upon air pollution in urban and sub-urban areas, Meteorol. Z., 15, 647–658, 2006.

Spindler, G., Müller, K., Brüggemann, E., Gnauk, T., and Herrmann, H.: Long-term size-segregated characterization of PM_{10}, $PM_{2.5}$, and PM_1 at the IfT research station Melpitz downwind of Leipzig (Germany) using high and low-volume filter samplers, Atmos. Environ., 38, 5333–5347, 2004.

Spindler, G., Brüggemann, E., Gnauk, T., Grüner, A., Müller, K., and Herrmann, H.: A four-year size-segregated characterization study of particles PM_{10}, $PM_{2.5}$ and PM_1 depending on air mass origin at Melpitz, Atmos. Environ., 44, 164–173, 2010.

The City of Leipzig; Air Quality Protection Plan (in German), http://www.forsten.sachsen.de/umwelt/download/luft/LRP2009_091218.pdf, 2009.

Sternbeck, J., Sjödin, Å., and Andréasson, K.: Metal emissions from road traffic and the influence of resuspension – results from two tunnel studies, Atmos. Environ., 36, 4735–4744, 2002.

Stohl, A.: Computation, accuracy and applications of trajectories – a review and bibliography, Atmos. Environ., 32, 947–966, 1998.

UBA: Trends in Air Quality in Germany, Federal Environment Agency (UBA), Dessau-Rosslau, Germany, 2009.

Vautard, R., Bessagnet, B., Chin, M., and Menut, L.: On the contribution of natural Aeolian sources to particulate matter concentrations in Europe: Testing hypotheses with a modelling approach, Atmos. Environ., 39, 3291–3303, 2005.

Velders, G. and Matthijsen, J.: Meteorological variability in NO_2 and PM_{10} concentrations in the Netherlands and its relation with EU limit values, Atmos. Environ., 43, 3858–3866, 2009.

Viana, M., Maenhaut, W., Chi, X., Querol, X., and Alastuey, A.: Comparative chemical mass closure of fine and coarse aerosols at two sites in south and west Europe: Implications for EU air pollution policies, Atmos. Environ., 41, 315–326, 2007.

Weckwerth, G.: Verification of traffic emitted aerosol components in the ambient air of Cologne (Germany), Atmos. Environ., 35, 5525–5536, 2001.

Wilcoxon, F.: Individual comparison by ranking methods, Biometrics Bull., 1, 80–83, 1945.

Wojcik, G. and Chang, J.: A re-evaluation of sulfur budgets, lifetimes, and scavenging ratios for Eastern North America, J. Atmos. Chem., 26, 109–145, 1997.

Yin, J. and Harrison, R.: Pragmatic mass closure study for $PM_{1.0}$, $PM_{2.5}$ and PM_{10} at roadside, urban background and rural sites, Atmos. Environ., 42, 980–988, 2008.